ADVANCES IN ATMOSPHERIC SCIENCES, VOL. 35, JANUARY 2018, 106–115

• **Original Paper** •

Record Low Sea-Ice Concentration in the Central Arctic during Summer 2010

Jinping ZHAO*[1], David BARBER[2], Shugang ZHANG[1], Qinghua YANG[3], Xiaoyu WANG[1], and Hongjie XIE[4]

[1]*Key Laboratory of Physical Oceanography, Ocean University of China, Qingdao,* 266100*, China*

[2]*Centre for Earth Observation Science, Faculty of Environment Earth and Resources, University of Manitoba, Winnipeg, Manitoba , R3T 2N2, Canada*

[3]*National Marine Environmental Forecasting Center, China, Beijing,* 100081*, China*

[4]*Department of Geological Sciences, University of Texas at San Antonio, San Antonio, Texas* 78284*, U.S.A.*

(Received 24 March 2017; revised 4 August 2017; accepted 5 September 2017)

ABSTRACT

The Arctic sea-ice extent has shown a declining trend over the past 30 years. Ice coverage reached historic minima in 2007 and again in 2012. This trend has recently been assessed to be unique over at least the last 1450 years. In the summer of 2010, a very low sea-ice concentration (SIC) appeared at high Arctic latitudes—even lower than that of surrounding pack ice at lower latitudes. This striking low ice concentration—referred to here as a record low ice concentration in the central Arctic (CARLIC)—is unique in our analysis period of 2003–15, and has not been previously reported in the literature. The CARLIC was not the result of ice melt, because sea ice was still quite thick based on in-situ ice thickness measurements. Instead, divergent ice drift appears to have been responsible for the CARLIC. A high correlation between SIC and wind stress curl suggests that the sea ice drift during the summer of 2010 responded strongly to the regional wind forcing. The drift trajectories of ice buoys exhibited a transpolar drift in the Atlantic sector and an eastward drift in the Pacific sector, which appeared to benefit the CARLIC in 2010. Under these conditions, more solar energy can penetrate into the open water, increasing melt through increased heat flux to the ocean. We speculate that this divergence of sea ice could occur more often in the coming decades, and impact on hemispheric SIC and feed back to the climate.

Key words: sea ice concentration, central Arctic, Beaufort Gyre, Transpolar Drift, ice motion, divergence

Citation: Zhao, J. P. , D. Barber, S. G. Zhang, Q. H. Yang, X. Y. Wang, and H. J. Xie, 2018: Record low sea-ice concentration in the central Arctic during summer 2010. *Adv. Atmos. Sci.*, **35**(1), 106–115, https://doi.org/10.1007/s00376-017-7066-6.

1. Introduction

Arctic sea-ice extent has been on the decline since the late 1970s (Lindsay and Zhang, 2005; Lemke et al., 2007), and has recently been assessed to be unique over at least a 1450-year period, including the relatively warm Medieval Period (Kinnard et al., 2011). The summer sea-ice extent underwent a decreasing trend in the past 30 years, at a rate of more than 70 000 km^2 yr^{-1} (Stroeve et al., 2007), and reached historic minima in summer 2007 (Comiso et al., 2008) and in 2012 (Overland and Wang, 2013). At this rate, a seasonally ice-free Arctic is expected sometime over the next few decades, according to a variety of models (e.g., Overland and Wang, 2007, 2013; Tietsche et al., 2011; Kay et al., 2011). The current metamorphosis from a multiyear-ice-dominated to a first-year-ice-dominated Arctic marine system appears to be a key feature of a warming planet (Lemke et al., 2007). With the reduction in multiyear ice, first-year ice has increased significantly in spatial extent and seasonal periodicity (Maslanik et al., 2011; Tschudi et al., 2016). The thinner ice and low sea-ice concentration (SIC) allow more absorption of solar radiation, which can increase the heat content of the ocean surface mixed layer (Perovich et al., 2008), and feeds back positively to more ice melt and increased energy and mass exchange across the ocean–sea-ice–atmosphere interface (Holland et al., 2006; Kumar et al., 2010, Raddatz et al., 2013).

The rapid decline in sea-ice extent and concentration has mostly been reported in terms of the significant change in the marginal ice zone (MIZ), which is a transitional zone between open ocean and pack ice (e.g., Stroeve et al., 2007). When the sea ice retreats and ice thickness reduces rapidly, the main feature of the ice concentration is the spread of the MIZ. The MIZ was historically a narrow zone, but has recently become much larger in extent. The low SIC area has become so wide that it may be becoming hard to distinguish the division between the MIZ and pack ice, throwing this historical definition into question. The perennial ice-extent loss is mainly caused by: ice advection toward the Canadian Archipelago coast; ice loading into the Transpolar Drift; acceleration of the Transpolar Drift carrying ice out of Fram Strait; and ice

* Corresponding author: Jinping ZHAO
Email: jpzhao@ouc.edu.cn

export to Baffin Bay through the Nares Strait (Nghiem et al., 2007).

Within the region north of 80°N—hereinafter referred to as the central Arctic—the SIC has remained high this century, with multiyear ice. However, the sea-ice age in the central Arctic has clearly responded to global warming. Most multiyear ice of age greater than ten years has been replaced by much younger ice (Belchansky et al., 2005). The loss of the oldest ice is even more extreme, with ice of greater than five years reaching a minimum in 2010 of just 6% of the 1983–2002 mean (Maslanik et al., 2011), illustrating that central Arctic ice has also been affected by this warming.

Here, we show the appearance of a record low ice concentration in the central Arctic (CARLIC) in summer 2010 based on field observations and satellite remote sensing. Large areas of open water appeared in high latitude areas, north of 85°N, resulting in a SIC that was actually lower than that of the surrounding pack ice at lower latitudes. This strikingly low ice concentration in the central Arctic is unique in our analysis period of 2003–15, and has not been previously reported in the literature. The remarkable opening of the ice appears not to have been produced by local melt, but rather by

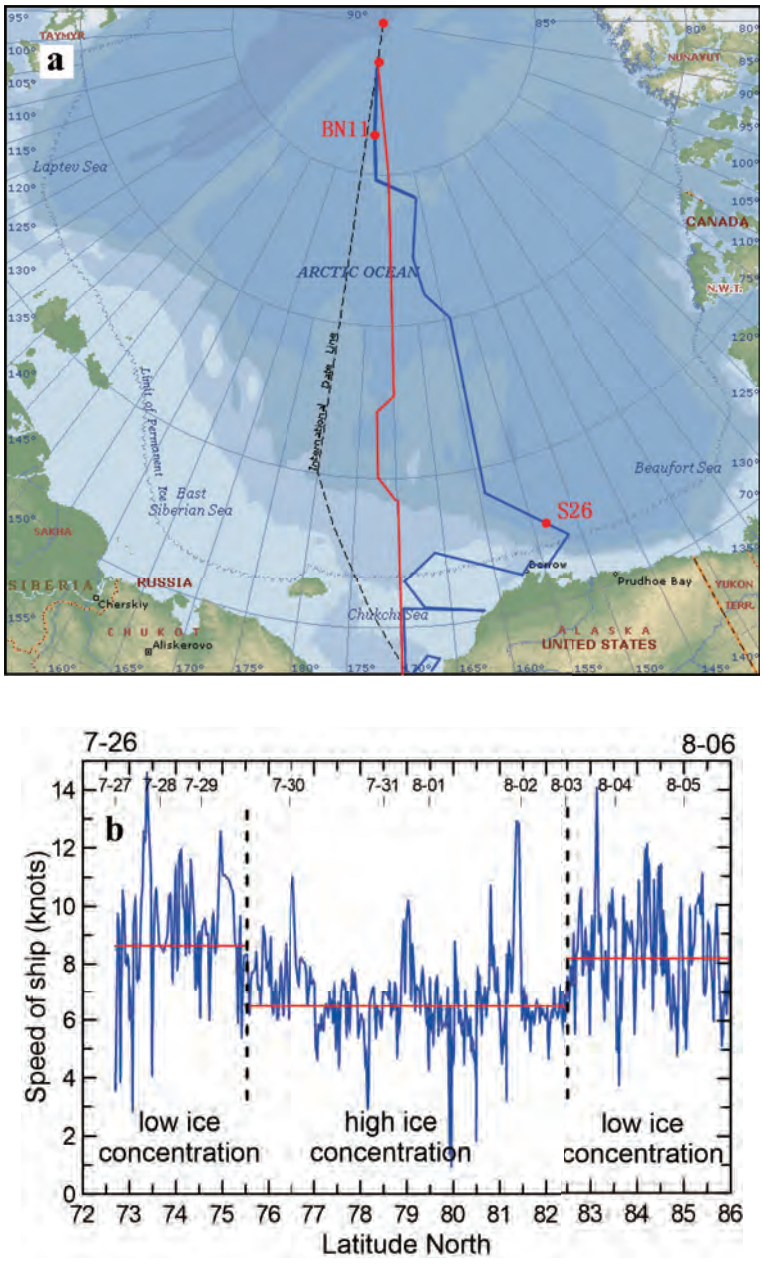

Fig. 1. Survey routes of *Xue Long* during its 2010 Arctic cruise. The blue line in (a) is the northward route and the red line the return route. (b) Navigation speed of the ship from 26 July to 6 August 2010, starting from Station S26 (72°42.04′N, 153°33.12′W) and ending at Station BN11 (86°04.85′N, 176°05.88′W). The red lines are latitudinally averaged navigation speed

sea-ice divergence. The objectives of this paper are to present new evidence for an observed reduction in SIC at high latitudes in the central high Arctic basin, and to ascertain what role regional-scale climate processes played in the observed processes.

2. Record low ice concentration zone

Very low ice concentration was first identified by the navigation speed of the Chinese R/V ship *Xue Long*. The ship started its northward journey from station S26 (72°42.04′N,

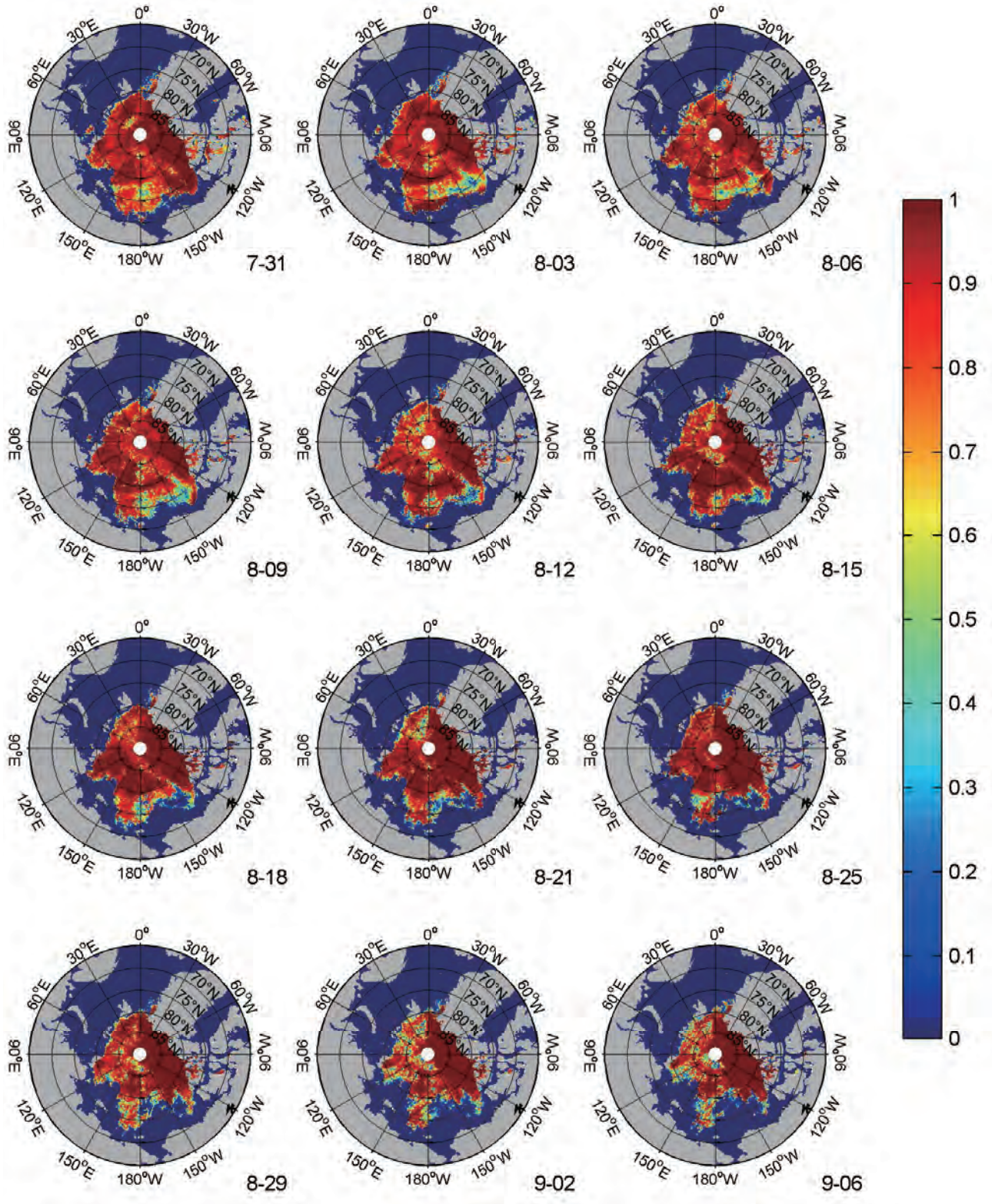

Fig. 2. Distribution of SIC in the Arctic Ocean during August 2010 from AMSR-E data. The white circle around the pole is defined here as the "North Pole blind zone", due to satellite orbital geometry.

153°33.12′W) on 27 July along the blue line in Fig. 1a. Ten days later, on 6 August, the ship arrived at Station BN11 (86°04.85′N, 176°05.88′W), from where the ship started ice camp measurements drifting with sea ice for 12 days. Ice conditions strongly influenced the navigation speed as the ship is an ice-strengthened ship, not an icebreaker. The ship traveled across a low SIC zone between 72.5°N and 75.6°N, with an average speed of 8.6 knots. Between 75.6°N and 82.6°N, the average navigation speed reduced to 6.5 knots, traveling in flat first-year ice of high concentration. From 82.6°N northward, the SIC decreased quickly and large areas of open water frequently appeared. The ship then traveled with an average navigation speed of more than 8.2 knots (Fig. 1b).

The spatial distribution of SIC could be determined from 89-GHz Advanced Microwave Scanning Radiometer-EOS (AMSR-E) daily satellite microwave data at 6.25-km resolution (http://www.iup.uni-bremen.de:8084/amsr/amsre.html). AMSR-E stopped working on 4 December 2011. Its successor—Advanced Microwave Scanning Radiometer 2 (AMSR2)—started to provide data from 18 May 2012. The SIC data are retrieved using the ARTIST Sea Ice algorithm (Spreen et al., 2008). The effects of melt ponds, wet snow and atmospheric water vapor can degrade SIC estimates, but SIC from AMSR-E reliably reflects the relative spatial difference of SIC (Meier, 2005). For convenience, we express SIC as a fraction of unity 0–1.

As shown in Fig. 2, a region with very low SIC centered at (83°N, 180°W) appeared on 31 July. It extended to a larger area up to the orbital "North Pole blind zone" of satellite coverage in the following 15 days. Although the low SIC area disappeared in the satellite record between 18 and 25 August, it subsequently reappeared, with the SIC reaching its minimum on 6 September.

The variation in low SIC in the central Arctic can be seen in the daily averaged SIC (ASIC),

$$\mathrm{ASIC}(t) = \frac{1}{S}\iint_S C(x,y,t)\,dx\,dy\,, \tag{1}$$

where $C(x,y,t)$ is the SIC at each grid point, and S is the area of the zone circled between a latitude (here, it is taken as 85°N) and the blind zone of satellite coverage (about 88.25°N). The variation in ASIC during 2003–15 from 1 August to 30 September is plotted in Fig. 3. It is shown that the ASIC was very high (> 0.9) in the central Arctic in most years. The lower ASICs appeared in 2007, 2010, 2012 and 2013. The minimum ASICs of the central Arctic dropped to about 0.87 (2007), 0.85 (2012) and 0.86 (2013). However, in 2010, the ASIC dropped abruptly to about 0.78, though the ice coverage of the whole Arctic was more than that in 2007 and 2012. The very low SIC in the central Arctic appeared in late July and existed continuously until late September. Figure 3 shows that the ASIC in early September was even lower than that encountered by the ship in early August 2010. As of the publication of this article, the record low of SIC in 2010 in the central Arctic has not been broken.

Here, we define a useful integral to express the interannual difference in SIC in the central Arctic:

$$\mathrm{AOW_{2M}} = \frac{1}{T}\int_0^T [1 - \mathrm{ASIC}(t)]\,dt\,, \tag{2}$$

where T is equal to 61 days within August and September, and $\mathrm{AOW_{2M}}$ is a two-month averaged area of open water.

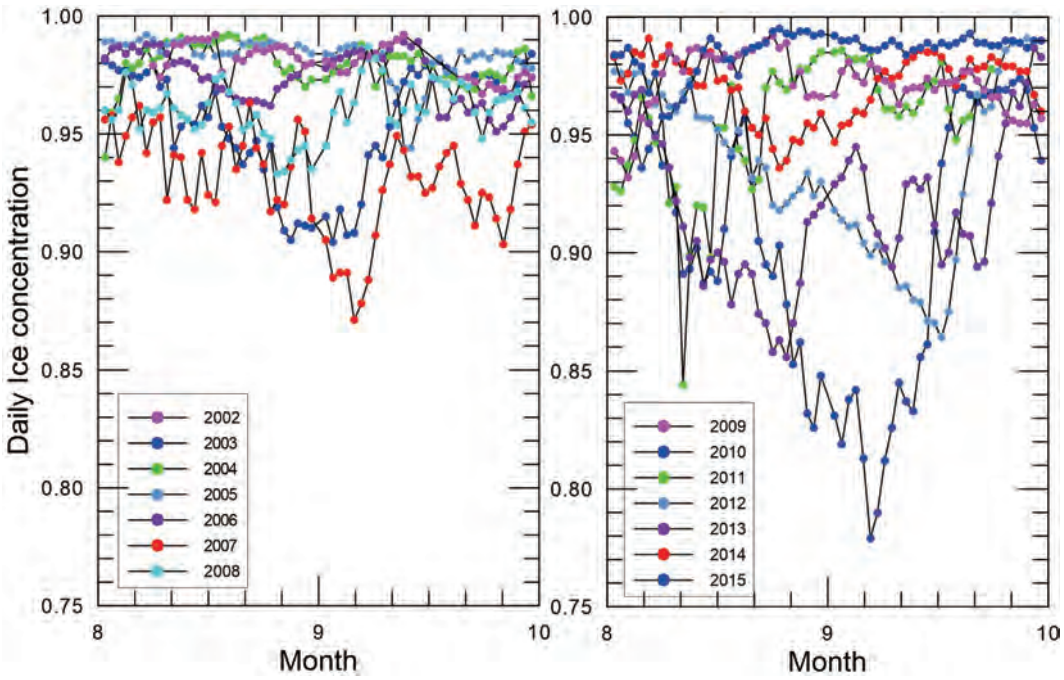

Fig. 3. Interannual features of low SIC in central Arctic. Daily average SIC north of 85°N from 1 August to 30 September from 2003 to 2015.

Higher values of AOW_{2M} indicate a joint effect of lower SIC and/or longer duration of the low ASIC. The AOW_{2M} for the central Arctic surrounded by 85°N in Fig. 4 clearly shows that the averaged area of open water reached its maximum in 2010 because of a longer-lasting low SIC. The AOW_{2M} in 2007 was the second lowest ASIC this century (Fig. 4). In 2012 and 2013, the minimum ASICs were close to that in 2007, but the AOW_{2M} in these years was much lower than that of 2007.

The two plots of SICs using the regional minimum days of 5 September 2007 and 6 September 2010 are plotted in Figs. 5a and b, respectively, to compare their differences. It is clear that the low overall concentration in 2007 was caused by an extreme retreat of the ice edge; whereas, within the pack ice, the concentration remained high (Fig. 5a). The low concentration in 2010 was different, as it formed as an opening within the pack ice (Fig. 5b). It can be seen from Fig. 5 that in 2010 not only did the SIC north of 85°N decline, but the overall SIC in the Atlantic sector was also significantly reduced.

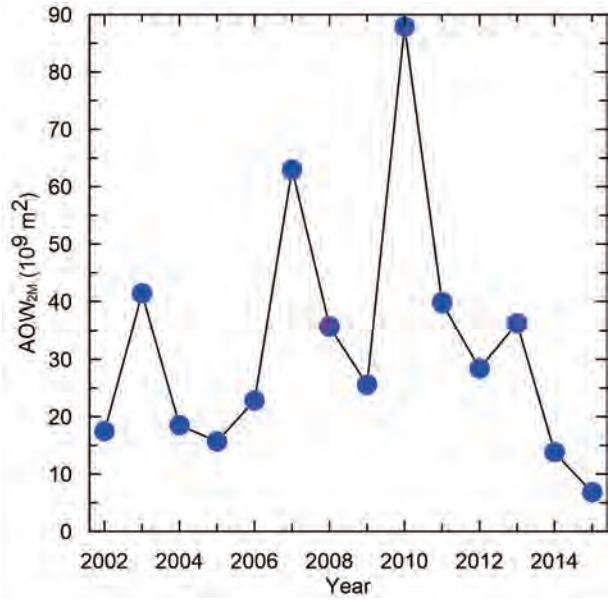

Fig. 4. Two-month averaged area of open water in the central Arctic surrounded by 85°N and the blind zone from 2003 to 2015.

3. Discussion on the driving factors of CARLIC

Based on optical measurements, Zhao et al. (2009) studied the sea-ice melt rate in the central Arctic. They found that only 0.33 cm d^{-1} of sea ice could be melted by absorption of solar radiation, even with the strong solar insolation in August. The solar radiation penetrating open water in the summer is the main heat source to the ocean surface mixed layer, as widely addressed by previous studies (e.g., Kadko and Swart, 2004). Work by Perovich et al. (2008) showed the strong influence of heat in the ocean surface mixed layer on the reduction of sea ice in the Beaufort Sea, while questioning whether the receipt of surface radiation would be able to melt ice at higher latitudes. Repeated in-situ ice thickness measurements by an electromagnetic induction (EM31) were conducted during the 12-day ice camp in 2010 started from (86°04.85′N, 176°05.88′W). The sea ice surrounding the ice camp was first-year ice, based on ice-core analysis (Lei et al., 2012). The measurements of ice thickness along four repeated profiles suggested an average melt rate of 2 cm d^{-1}, primarily bottom melt (Xie et al., 2013). The melting rate was 2.5 times greater than the average ~ 0.8 cm d^{-1} during a similar period of the SHEBA experiments in 1998, even though SHEBA was at much lower latitudes (70°–80°N) (Perovich et al., 2003). The high melt rate occurred due to the heat absorption through the large area of open water. However, even with this rate, it would still need 100 days to melt a 2-

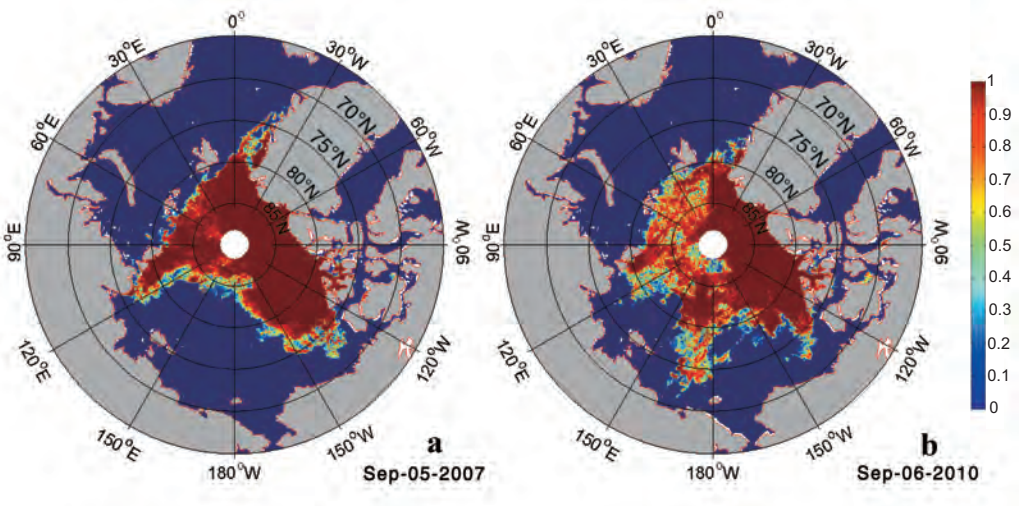

Fig. 5. Distribution of ice concentration in the Arctic Ocean with the lowest daily average SIC north of 85°N in (a) 2007 and (b) 2010.

m-thick layer of ice. Therefore, the sea-ice melt could not be solely responsible for the record low SIC at the end of July. Instead, the rapid opening and closing shift of the low SIC region suggests that the divergence/convergence of ice drift might be more relevant to the CARLIC.

The transfer of momentum from the atmosphere to the ice is critical to sea-ice drift (Martin and Gerdes, 2007). Ignoring the geopotential gradient and nonlinear interaction, the equation of ice motion as a continuum is (Leppäranta, 2005)

$$\rho h\left(\frac{\partial \boldsymbol{v}}{\partial t}+f\boldsymbol{k}\times\boldsymbol{v}\right)=\nabla\cdot\boldsymbol{\sigma}+\boldsymbol{\tau}_{\mathrm{a}}+\boldsymbol{\tau}_{rmw}\,, \tag{3}$$

where $\boldsymbol{v}$ is ice velocity; ρ is sea ice density; h is ice thickness; f is the Coriolis parameter; $\boldsymbol{\sigma}$ is the two-dimensional internal ice stress; $\boldsymbol{\tau}_{\mathrm{a}}$ and $\boldsymbol{\tau}_{\mathrm{w}}$ are the wind and water stresses acting on the upper and bottom surfaces of sea ice. Provided ρ and h are locally homogeneous, the divergence of ice drift, D, and relative vorticity, ζ,

$$D=\frac{\partial u}{\partial x}+\frac{\partial v}{\partial y};\quad \zeta=\frac{\partial v}{\partial x}-\frac{\partial u}{\partial y}\,,$$

can be obtained by taking the curl and divergence for both sides of Eq. (3):

$$\begin{aligned}\rho h\left(\frac{\partial \zeta}{\partial t}+fD\right)&=\nabla\times\nabla\cdot\boldsymbol{\sigma}+\mathrm{curl}\boldsymbol{\tau}_{\mathrm{a}}+\mathrm{curl}\boldsymbol{\tau}_{\mathrm{w}}\\ \rho h\left(\frac{\partial D}{\partial t}-f\zeta\right)&=\nabla(\nabla\cdot\boldsymbol{\sigma})+\mathrm{div}\boldsymbol{\tau}_{\mathrm{a}}+\mathrm{div}\boldsymbol{\tau}_{\mathrm{w}}\end{aligned}\,. \tag{4}$$

Then, the equation for the divergence of ice drift is

$$\begin{aligned}\rho h\left(\frac{\partial^2 D}{\partial t^2}+f^2D\right)&=f[\nabla\times(\nabla\cdot\boldsymbol{\sigma})+(\mathrm{curl}\boldsymbol{\tau}_{\mathrm{a}}+\mathrm{curl}\boldsymbol{\tau}_{\mathrm{w}})]\\&\quad+\frac{\partial}{\partial t}[\nabla(\nabla\cdot\boldsymbol{\sigma})+(\mathrm{div}\boldsymbol{\tau}_{\mathrm{a}}+\mathrm{div}\boldsymbol{\tau}_{\mathrm{w}})]\,.\end{aligned} \tag{5}$$

Considering that the time scale of ice drifting is larger than the inertial period, the two-order temporal derivative is small, and the variation of the divergence of the stresses is negligible, through analyzing the order of magnitude, D can be approximately expressed by

$$D\approx\frac{1}{\rho f h}[\nabla\times(\nabla\cdot\boldsymbol{\sigma})+(\mathrm{curl}\boldsymbol{\tau}_{\mathrm{a}}+\mathrm{curl}\boldsymbol{\tau}_{\mathrm{w}})]\,. \tag{6}$$

The equation of ice concentration is as follows (Hibler, 1979):

$$\frac{\partial C}{\partial t}=-\left(\frac{\partial uC}{\partial x}+\frac{\partial vC}{\partial y}\right)+S_A+\varepsilon\,, \tag{7}$$

where S_A is related to ice growth, and ε represents diffusion terms. Because the new ice formation is negligible in this season, and the diffusion and advection are both small, the relationship between the divergence of sea-ice drift and concentration becomes

$$\frac{\partial C}{\partial t}=-CD\,. \tag{8}$$

Replacing D with a spatially averaged version in the region north of 85°N, and substituting Eq. (8) into Eq. (1), we obtain

$$\frac{1}{\mathrm{ASIC}(t)}\frac{d\mathrm{ASIC}(t)}{dt}\approx-\frac{1}{\rho f h S}\iint_S(\nabla\times(\nabla\cdot\boldsymbol{\sigma})+\mathrm{curl}\boldsymbol{\tau}_{\mathrm{a}}+\mathrm{curl}\boldsymbol{\tau}_{\mathrm{w}})ds, \tag{9}$$

where S is the area north of 85°N, and the left-hand side of Eq. (9) is the relative rate of variation of ASIC. Because the internal ice stress and the drag stress of water are unknown, ASIC(t) cannot be obtained from Eq. (9). The response of the variation in SIC depends on the SIC itself. When sea ice is dense, the sea ice responds weakly to the wind stress curl, as the internal stress $\boldsymbol{\sigma}$ arising from the interaction of different parts of ice floe balance most of the wind forcing. Otherwise, when the sea ice is sparse, the ice drift becomes more responsive to wind (Kwok et al., 2013; Olason and Notz, 2014). The water drag stress for sea ice usually responds to ice drift. The curl of wind stress in this equation is the only forcing factor, and the other terms are response factors and are expected to respond to the wind in different ways.

We calculated the daily averaged wind stress curl (AWSC) north of 85°N in August and September 2010 using daily wind velocity data from NCEP Reanalysis 1 (Kalnay et al., 1996). The relative rate of variation of ASIC was calculated using the daily ASIC. The total correlation coefficient between ASIC and AWSC was −0.54, at much higher than the 99.5% confidence level. It can be seen from Fig. 6a that ASIC responds well to each event with high averaged wind stress curl. It verifies that the wind stress curl is one of the most important factors in producing CARLIC.

Although the relative rate of variation of ASIC correlated well with wind stress curl, the response of ASIC itself to wind stress curl was related to the degree of sea-ice concentrating, as shown in Fig. 6b. From early August, a positive AWSC lasted for a couple of weeks, driving the ASIC decline from 0.97 to its first minimum of 0.89. Then, a seven-day negative AWSC acted on the area to cause a convergence of the ice-drift field, and the ASIC recovered to 0.96. After this, a three-week period dominated by positive AWSC occurred. The ASIC declined again and reached its minimum of 0.78 on 6 September. A rapid increase in the ASIC occurred again, responding to the strong negative trend of AWSC since 13 September, and all of the open water in the central Arctic closed over this period. The positive AWSC occurred once again after 20 September, but the ASIC did not respond to it anymore because freezing of sea ice had begun at these high latitudes.

The AWSCs of August in recent years are plotted in Fig. 7. Since 2007, the wind stress curl in the central Arctic was negative, except in 2010. This may explain why the CARLIC only occurred in 2010. During the sea-ice minimum in 2007, the amount of multiyear ice was reduced in the Pacific sector of the Arctic Ocean, and replaced with an increased areal extent of first-year ice (Barber et al., 2012). With positive wind stress curl, the ASIC in 2007 reached the second low record. In 2012 summer, the sea-ice cover of the Arctic reached its recorded minimum, but the ice concentration in the central

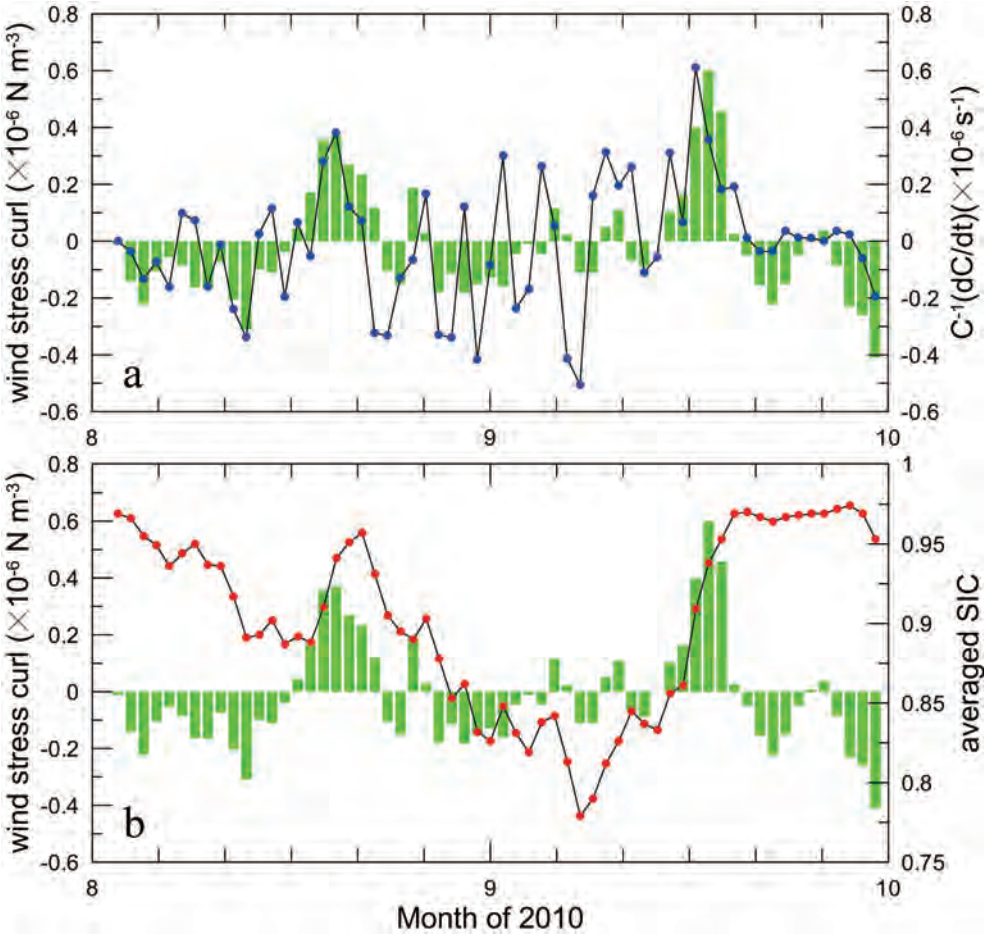

Fig. 6. Influence of wind stress curl on SIC. The green bars present the time series of negative averaged wind stress curl (AWSC) north of 85°N. (a) Correlation of AWSC and relative rate of variation of ASIC (blue dots). The correlation coefficient is −0.54. (b) Comparison of AWSC and ASIC (red dots).

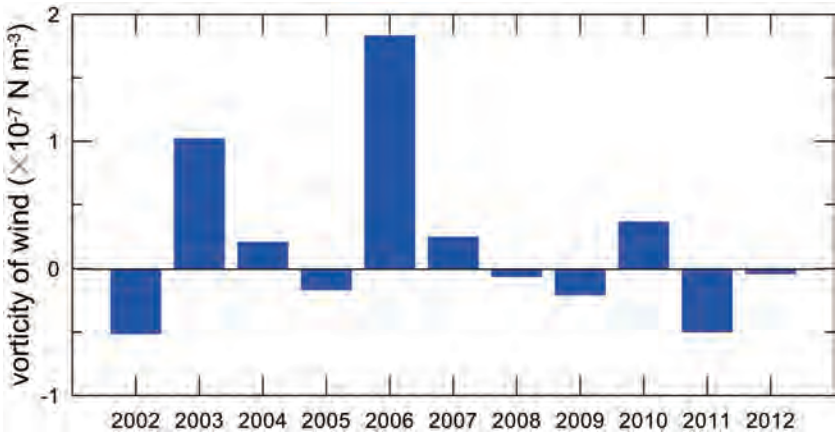

Fig. 7. Averaged wind stress curl in August each year.

Arctic was still high. This means that the wind stress curl did not drive the occurrence of low SIC in the central Arctic after 2010.

However, in 2003 and 2006, positive wind stress curls with magnitudes much larger than those in 2007 and 2010 were found, but no CARLIC events occurred. Therefore, it seems that the wind forcing is not the only factor in generating CARLIC. A reasonable explanation is that the SIC in 2003 and 2006 was higher (see Fig. 3), responding poorly to wind forcing. The response of the ice to wind forcing has recently become more pronounced, since in summer the Arctic is now dominated by first-year ice types, smaller floe sizes

and decreased concentration (e.g., Asplin et al., 2009), allowing for increased ice speeds within the gyres (Galley et al., 2013).

Besides the regional wind forcing by positive wind stress curl, the ice drift patterns on the basin scale might also contribute to the CARLIC. The trajectories of the buoys from the International Arctic Buoy Program (IABP; Rigor, 2002) from 1 January to 30 September 2010 (Fig. 8a) were clustered into two regions, separated by the dashed purple line: one group went toward the Fram Strait within the Transpolar Drift, and the other went eastward into the Beaufort Gyre. No buoy went across the dashed line in the first 10 months of 2010, which means that the ice flowing out of the Arctic was partly compensated for by export from the Laptev Sea and western sector. The lack of full compensation favored a low ice concentration.

The averaged SLP field of April to August 2010 (Fig. 8b) also matches the drift patterns identified from the IABP buoys. This pattern drives the production of a divergence in the central Arctic, which is quite similar to the double-gyre ice drift pattern reported by Wang and Zhao (2012). Using Polar Pathfinder monthly 25-km EASE-Grid Sea Ice Motion Vectors (Fowler, 2008), Wang and Zhao (2012) divided the ice drift pattern into four main types: Transpolar Drift plus Beaufort Gyre (TPDBG; 38% of total occurrence), anticyclonic (15%), cyclonic (16%), and double-gyre (15%). The TPDBG type is the typical ice drift pattern in the Arctic, with the highest occurrence. The double-gyre drift type is quite similar to the TPDBG type, except that the sea ice in the central Arctic drifts to the Canadian Archipelago, not to the Fram Strait—quite similar to the typical characteristic of the drifting pattern in 2010. Although the double-gyre drift pattern benefits divergence in the central Arctic, its occurrence usually lasts a short time. However, in 2010, the double-gyre pattern at the basin scale lasted more than 10 months, which might have been the immediate cause of the CARLIC.

4. Summary and conclusions

A record low concentration of sea ice and large area of open water in the central Arctic during summer 2010 is reported in this paper. The lowest averaged SIC north of 85°N reached as low as 0.78, becoming the sparsest than at any time in the historical record. We conclude that, in this particular case, the low SIC was caused more by ice divergence than by in-situ melt, based on the temporally resolved measurement of ice melt at a nearby ice camp. A high correlation between SIC and wind stress curl is revealed to address the contribution of regional wind forcing on the divergence of ice drift. The high correlation coefficient suggests that regional wind forcing might have been a key driving factor of the sea-ice drift in summer 2010. However, in 2003 and 2006, the magnitude of the wind stress curls were much larger than those in 2007 and 2010, but no CARLIC events occurred, because the heavy ice seems to have prevented the occurrence of low SIC, as the region was still dominated then by multiyear ice forms. The drift trajectories of ice buoys (IABP) depicted a divergent transpolar drift in the Atlantic sector and an eastward drift in the Pacific sector. This feature illustrates a double-gyre drift pattern, cyclonic in the Transpolar Drift and anticyclonic in the Beaufort Gyre, which resulted in ice divergence in the central Arctic. In 2010, this drift pattern resulted in high concentrations of sea ice at lower latitudes, which decreased within the high latitudes toward the pole (Fig. 1). This pattern was also observed in 2009 (Barber et al., 2009), and again in 2012 (Babb et al., 2013), while the occurrence in 2010 lasted more than 10 months and the persistent divergence drove CARLIC.

An important question relates to the frequency of future occurrences of CARLIC-type events in the central Arctic,

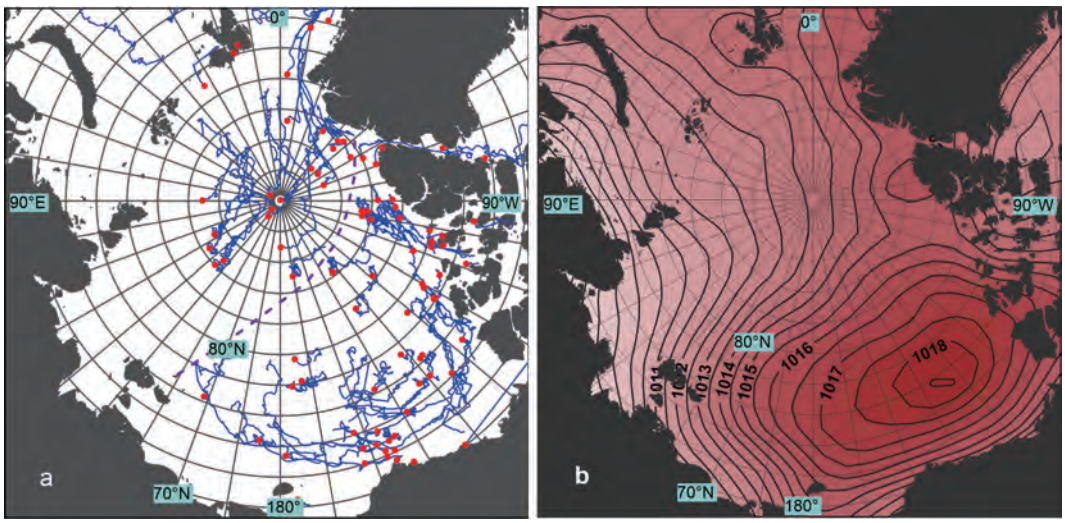

Fig. 8. Ice-drift pattern in 2010. (a) Drift trajectories of ice buoys in the Arctic Ocean from 1 January to 30 September 2010. Red dots are the start positions of each buoy. The dashed purple line is the division of the two drifting groups. (b) Averaged SLP of April–August 2010.

which is difficult to project given its rare occurrence and our limited knowledge about their formation and maintenance. Based on our results, however, a long-lasting positive wind stress curl favors the occurrence of CARLIC, which might occur again when such a wind condition reappears. This divergence of ice drift in the central Arctic might be a significant feature of sea-ice rapid decline at high latitudes in the future, due to the preconditioning that the open water would have on increasing melt from an enhanced ocean surface mixed layer temperature. The physical significance of CARLIC is that more solar energy can penetrate into open water, which can in turn enhance the ice melt and feed back to the atmosphere (Vihma, 2014). The large area of open water in the ice pack potentially has substantial biological implications as well. Further investigation is necessary to reveal the climatic significance of this double-gyre pattern, and its coupling to sea-ice motion and melt.

Acknowledgements. This study was funded by the Global Change Research Program of China (Grant No. 2015CB953900), the Key Program of the National Natural Science Foundation of China (Grant Nos. 41330960 and 41406208), the Canada Research Chairs Program, NSERC, and Canadian Federal IPY Program Office. This paper is a contribution to the Arctic Science Partnership (ASP) and ArcticNet research networks.

REFERENCES

Asplin, M. G., J. V. Lukovich, and D. G. Barber, 2009: Atmospheric forcing of the Beaufort Sea Ice Gyre: Surface pressure climatology and sea ice motion. *J. Geophys. Res.*, **114**, C00A06, https://doi.org/10.1029/2008JC005127.

Babb, D., R. J. Galley, M. G. Asplin, J. V. Lukovich, and D. G. Barber, 2013: Multiyear sea ice export through the Bering Strait during winter 201112. *J. Geophys. Res.*, **118**, 5489-5503, https://doi.org/10.1002/jgrc.20383.

Barber, D. G., and Coauthors, 2009: Perennial pack ice in the southern Beaufort Sea was not as it appeared in the summer of 2009. *Geophys. Res. Lett.*, **36**, L24501, https://doi.org/10.1029/2009GL041434.

Barber, D. G., and Coauthors, 2012: Change and variability in sea ice during the 2007-2008 Canadian International Polar Year Program. *Climatic Change*, **115**, 115–133, https://doi.org/10.1007/s10584-012-0477-6.

Belchansky, G. I., D. C. Douglas, and N. G. Platonov, 2005: Spatial and temporal variations in the age structure of Arctic sea ice. *Geophys. Res. Lett.*, **32**, L18504, https://doi.org/10.1029/2005GL023976.

Comiso, J. C., C. L. Parkinson, R. Gersten, and L. Stock, 2008: Accelerated decline in the Arctic sea ice cover. *Geophys. Res. Lett.*, **35**, L01703, https://doi.org/10.1029/2007GL031972.

Fowler, C., 2008: Polar Pathfinder Daily 25 km EASE-Grid Sea Ice Motion Vectors. National Snow and Ice Data Center, Boulder, Colorado USA. Digital Media.

Galley, R. J., B. G. T. Else, S. J. Prinsenberg, and D. G. Barber, 2013: Summer sea ice concentration, motion, and thickness near areas of proposed offshore oil and gas development in the Canadian Beaufort Sea-2009. *Arctic*, **66**(1), 105–116.

Hibler III, W. D., 1979: A dynamic thermodynamic sea ice model. *J. Phys. Oceanogr.*, **9**, 815–846, https://doi.org/10.1175/1520-0485(1979)009<0815:ADTSIM>2.0.CO;2.

Holland, M. M., C. M. Bitz, E. C. Hunke, W. H. Lipscomb, and J. L. Schramm, 2006: Influence of the sea ice thickness distribution on polar climate in CCSM3. *J. Climate*, **19**(11), 2398–2414, https://doi.org/10.1175/JCLI3751.1.

Kadko D., and P. Swart, 2004: The source of the high heat and freshwater content of the upper ocean at the SHEBA site in the Beaufort Sea in 1997. *J. Geophys. Res.*, **109**, C01022, https://doi.org/10.1029/2002JC001734.

Kalnay, E., and Coauthors, 1996: The NCEP/NCAR 40-year reanalysis project. *Bull. Amer. Meteor. Soc.*, **77**(3), 437–471, https://doi.org/10.1175/1520-0477(1996)077<0437:TNYRP>2.0.CO;2.

Kay, J. E., M. M. Holland, and A. Jahn, 2011: Inter-annual to multi-decadal Arctic sea ice extent trends in a warming world. *Geophys. Res. Lett.*, **38**, L15708, https://doi.org/10.1029/2011GL048008.

Kinnard, C., C. M. Zdanowicz, D. A. Fisher, E. Isaksson, A. de Vernal, and L. G. Thompson, 2011: Reconstructed changes in Arctic sea ice over the past 1,450 years. *Nature*, **479**, 509–512, Https://doi.org/10.1038/nature10581.

Kumar, A., and Coauthors, 2010: Contribution of sea ice loss to Arctic amplification. *Geophys. Res. Lett.*, **37**, L21701, https://doi.org/10.1029/2010GL045022.

Kwok, R., G. Spreen, and S. Pang, 2013: Arctic sea ice circulation and drift speed: Decadal trends and ocean currents. *J. Geophys. Res.*, **118**, 2408–2425, https://doi.org/10.1002/jgrc.20191.

Lei, R. B., Z. H. Zhang, I. Matero, B. Cheng, Q. Li, and W. F. Huang, 2012: Reflection and transmission of irradiance by snow and sea ice in the central Arctic Ocean in summer 2010. *Polar Research*, **31**, 17325, https://doi.org/10.3402/polar.v31i0.17325.

Lemke, P., and Coauthors, 2007: Observations: Changes in snow, ice and frozen ground. *Climate Change 2007: The Physical Science Basis. Contribution of Working Group I to the Fourth Assessment Report of the Intergovernmental Panel on Climate Change*, Soloon et al., Eds. Cambridge University Press, Cambridge, United Kingdom and New York, USA, 339–383.

Leppäranta, M., 2005: *The Drift of Sea Ice*. Springer-Verlag, 266 pp.

Lindsay, R. W., and J. Zhang, 2005: The thinning of Arctic sea ice, 1988-2003: have we passed a tipping point? *J. Climate*, **18**(22), 4879–4894, https://doi.org/10.1175/JCLI3587.1.

Martin, T., and R. Gerdes, 2007: Sea ice drift variability in Arctic Ocean Model Intercomparison Project models and observations. *J. Geophys. Res.*, **112**, C04S10, https://doi.org/10.1029/2006JC003617.

Maslanik, J. A., J. Stroeve, C. Fowler, and W. Emery, 2011: Distribution and trends in Arctic sea ice age through spring 2011. *Geophys. Res. Lett.*, **38**, L13502, https://doi.org/10.1029/2011GL047735.

Meier, W. N., 2005: Comparison of passive microwave ice concentration algorithm retrievals with AVHRR imagery in Arctic peripheral seas. *IEEE Transactions on Geoscience and Remote Sensing*, **43**(7), 1324–1337, https://doi.org/10.1109/TGRS.2005.846151.

Nghiem, S. V., I. G. Rigor, D. K. Perovich, P. Clemente-Colón, J. W. Weatherly, and G. Neumann, 2007: Rapid reduction of Arctic perennial sea ice. *Geophys. Res. Lett.*, **34**, L19504, https://doi.org/10.1029/2007GL031138.

Olason, E., and D. Notz, 2014: Drivers of variability in Arctic sea-ice drift speed. *J. Geophys. Res.*, **119**, 5755–5775, https://doi.org/10.1002/2014JC009897.

Overland, J. E., and M. Y. Wang, 2007: Future regional Arctic sea ice declines. *Geophys. Res. Lett.*, **34**, L17705, https://doi.org/10.1029/2007GL030808.

Overland, J. E., and M. Y. Wang, 2013: When will the summer Arctic be nearly sea ice free? *Geophys. Res. Lett.*, **40**, 2097–2101, https://doi.org/10.1002/grl.50316.

Perovich, D. K., T. C. Grenfell, J. A. Richter-Menge, B. Light, W. B. Tucker III, and H. Eicken, 2003: Thin and thinner: Sea ice mass balance measurements during SHEBA. *J. Geophys. Res.*, **108**(C3), 8050, https://doi.org/10.1029/2001JC001079.

Perovich, D. K., J. A. Richter-Menge, K. F. Jones, and B. Light, 2008: Sunlight, water, and ice: Extreme Arctic sea ice melt during the summer of 2007. *Geophys. Res. Lett.*, **35**, L11501, https://doi.org/10.1029/2008GL034007.

Raddatz, R. L., R. J. Galley, L. M. Candlish, M. G. Asplin, and D. G. Barber, 2013: Integral profile estimates of latent heat flux under clear skies at an unconsolidated sea-ice surface. *Atmos.-Ocean.*, **51**(3), 239–248.

Rigor, I., 2002: IABP drifting buoy pressure, temperature, position, and interpolated ice velocity. Compiled by the Polar Science Center, Applied Physics Laboratory, University of Washington, Seattle, in association with NSIDC. National Snow and Ice Data Center, Boulder, CO, https://dx.doi.org/10.7265/N53X84K7.

Spreen, G., L. Kaleschke, and G. Heygster, 2008: Sea ice remote sensing using AMSR-E 89-GHz channels. *J. Geophys. Res.*, **113**, C02S03, https://doi.org/10.1029/2005JC003384.

Stroeve, J., M. M. Holland, W. Meier, T. Scambos, and M. Serreze, 2007: Arctic sea ice decline: Faster than forecast. *Geophys. Res. Lett.*, **34**, L09501, https://doi.org/10.1029/2007GL029703.

Tietsche, S., D. Notz, J. H. Jungclaus, and J. Marotzke, 2011: Recovery mechanisms of Arctic summer sea ice. *Geophys. Res. Lett.*, **38**, L02707, https://doi.org/10.1029/2010GL045698.

Tschudi, M. A., J. C. Stroeve, and J. S. Stewart, 2016: Relating the age of Arctic Sea ice to its thickness, as measured during NASA's ICESat and IceBridge campaigns. *Remote Sensing*, **8**, 457, https://doi.org/10.3390/rs8060457.

Vihma, T., 2014: Effects of Arctic sea ice decline on weather and climate: A review. *Surveys in Geophysics*, **35**, 1175–1214, https://doi.org/10.1007/s10712-014-9284-0.

Wang, X. Y., and J. P. Zhao, 2012: Seasonal and inter-annual variations of the primary types of the Arctic sea-ice drifting patterns. *Advances in Polar Science*, **23**(2): 72–81, https://doi.org/10.3724/SP.J.1085.2012.00072.

Xie, H., R. Lei, C. Ke, H. Wang, Z. Li, J. Zhao, and S. F. Ackley, 2013: Summer sea ice characteristics and morphology in the Pacific Arctic sector as observed during the CHINARE 2010 cruise. *The Cryosphere*, **7**, 1057–1072, https://doi.org/10.5194/tc-7-1057-2013.

Zhao, J. P, T. Li, S. G. Zhang, and Y. T. Jiao, 2009: The shortwave solar radiation energy absorbed by packed sea ice in the central Arctic. *Advances in Earth Science*, **24**(1), 34–42, https://doi.org/10.3321/j.issn:1001-8166.2009.01.004. (in Chinese with English abstract)